An efficient loudspeaker horn designed by numerical optimization: an experimental study

D. Noreland*, R. Udawalpola**, P. Seoane***
E. Wadbro*, M. Berggren*
*Department of Computing Science, Umeå University
**Department of Information Technology, Uppsala University
***D.A.S. Audio S.A., Valencia, Spain

Report UMINF 10.1
Department of Computing Science
Umeå University
901 87 Umeå, Sweden

January 2010

Abstract

Using rapid prototyping, we manufacture an acoustic horn designed by gradient-based shape optimization to have virtually perfect impedance-matching properties. The horn is 161.5 mm long, has a mouth diameter of 300 mm, and a throat diameter intended for a 1.5 inch driver. We optimize the horn with the aim of having perfect radiation efficiency at 31 frequencies in the range 1.6–9.05 kHz, while satisfying a convexity constraint on the flare. The acoustical properties, as needed by the optimization algorithm, are calculated through numerical solutions with the finite-element method of the axisymmetric Helmholtz equation. The prototype has been analyzed in an anechoic chamber. In the design frequency band, the acoustic input impedance agrees reasonably well with the ideal characteristic impedance of a waveguide with the same cross sectional area as the horn throat.

1 Introduction

The horn loudspeaker was the first loudspeaker that was successfully used for public address (PA) systems. The horn concept, or variations/extensions of it, such as the assembly into line arrays, remains a popular solution also today, but its acoustical properties are not always preferred due to its sound quality that is sometimes perceived as “honky” or “funnel like”. Some of the disadvantages of horn loudspeakers may, however, be attributed to suboptimal design and are not necessarily due to inherent properties of the acoustical horn. It should be borne in mind that different acoustical horns serve diametrically opposed purposes.

The horn found in brass wind instruments is a part of a resonator (which actually *minimizes* the radiation capacity precisely at the resonating frequencies), whereas the loudspeaker horn has the opposite purpose: to radiate sound as efficiently as possible over as wide a frequency band as possible. For a loudspeaker it is desirable to reduce resonances, since those may affect the performance of the loudspeaker adversely. Resonances assign various formants to the horn, which in effect is perceived as a coloring of the signal. By the use of linear filters, such effects can be counteracted, but each PA-system has to be tuned individually. With a matched horn, the internal sound pressure level (SPL) is kept down for a given external SPL, and this may possibly be advantageous to the non-linear distortion properties of the loudspeaker. The non-linear effects occur due to the finite amplitude of the acoustic waves, as well as the non-linearity of the suspension of the diaphragm. Another significant source of non-linear distortion is when the volume change of the compression chamber as the diaphragm moves is not negligible compared to the equilibrium volume.

The unsuccessful design of some horn loudspeakers can be attributed to the fact that the driver and the horn have not been matched to each other. A careful design of a horn loudspeaker should ideally not treat the driver and the horn separately; it would be desirable to optimize simultaneously the internal geometry of the driver and the horn shape. However, if higher-mode excitation is small in the junction between driver and horn, the design process becomes modular in the sense that once a horn with a real and constant impedance spectrum has been computed, a matching phaser plug can be designed in a subsequent step. Or, conversely, given an existing driver, an optimal acoustic loading of the driver can be determined in a first step. The spectrum corresponding to this optimal loding could then be used as a target input impedance for the horn in a second shape optimization run. The present report should be regarded as a first step in such a program. It constitutes a concept study in that a very specific issue—the maximization of transmission efficiency—is addressed. A natural, and in a real loudspeaker design case necessary, extension would be to optimize also with respect to the loudspeakers directivity properties.

It is hoped that the results of the present paper be valuable to related applications, either as a source of inspiration or offering more immediately applicable results. For instance, a horn optimized for maximum transmission efficiency simulates a perfect absorber. Such a device is a central component in measurement systems for bore reconstruction of musical instruments based on pulse reflectometry [5]. Such dampers are presently implemented by very long tubes (50–100 m), relying on the internal damping in the tube. For a system of small internal diameter, this is not a problem since the tube is readily coiled and damping is high (0.11 dB/m at 200 Hz for a 7.8 mm tube), but a wider tube is both much harder to handle and provides significantly lower damping (doubling the diameter approximately halves the damping), which further increases the required length. The *impedance matching cone* in the aforementioned system is a contracting horn connecting the large-diameter loudspeaker, responsible for the

generation of a pulse, to a tube of the (small) input diameter of the object to be investigated. Such an impedance transformer is in principle akin to the matched loudspeaker horn, and could be designed using the tools employed in the present work.

2 The design problem

The present work utilizes previously developed methods [1, 7], where numerical optimization algorithms have been applied to the design of loudspeaker horn. The aim is to find a horn profile within a large search space of admissible designs that optimizes the performance of the horn with respect to its transmission properties, as measured in the horn throat. Only a limited set of constraints, mainly related to manufacturing issues, are imposed; instead of working with a relatively small number of variables in a parameterization (for instance the control points of a spline curve), design variations that act in principle on the grid resolution level are allowed. In this way, it is possible to find shapes with corners or other features that may be difficult to foresee when choosing more restrictive parameterizations.

The angular variation of the exterior sound field is of course of great interest for a PA system. One of the advantages of horn loudspeakers is their comparatively homogeneous field, without pronounced fringes or split central lobes, etc. Previous experience [7] of directivity optimization through flare adjustments of axisymmetric horns indicates that the far field directivity can be controlled only at the expense of a serious penalty on the transmission efficiency. It is thus likely that a larger design space, such as real 3D shapes, and/or additional diffractive devices are needed to obtain both high transmission efficiency and good control of the directivity properties. A first step in that direction has recently been attempted by considering design optimization of an horn/acoustic lens combination in a planar 2D setting [8].

The underlying physical model is the wave equation in two dimensions. By choosing an axisymmetric geometry, the model is effectively three-dimensional and takes higher acoustical radial (but not circumferential) modes into consideration. The equations are solved using a finite element method on a computational mesh that conforms to the horn contour. This means that at each design cycle, the computational mesh needs to be modified, and the finite element solution is recomputed for a set of frequencies suitable distributed over a design frequency band. Due to the computationally intensive model, it is necessary to use an optimization algorithm that makes efficient use of the computed solution and its properties. The large sensitivity of acoustic problems to geometrical shapes makes gradient-based optimization schemes an excellent choice. By the use of the so-called adjoint technique [4], it is possible to compute the gradient of the objective function at a cost that is roughly similar to that of a forward solution, regardless of the number of design parameters. The success of the method de-

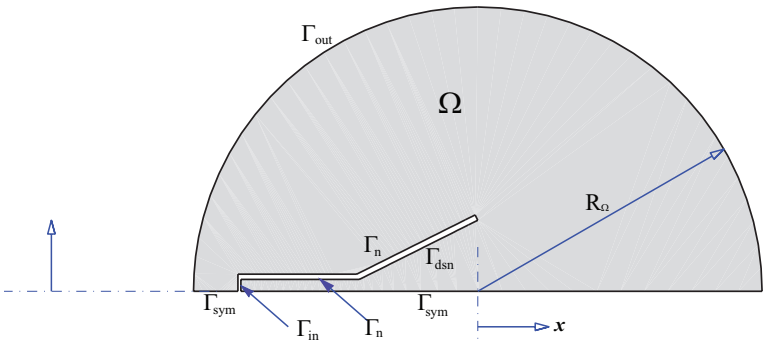

Figure 1: The computational domain and the representation of the geometry of the horn.

pends on several factors, such as the ability to smoothly distribute boundary deformations to the interior points of the computational mesh while keeping the mesh topology fixed [1, 7].

2.1 Mathematical model

The exterior domain of propagation is truncated to a bounded domain Ω, as illustrated in Fig. 1, to facilitate the numerical treatment. To model the exterior propagation of a wave with wave number k, we solve the following boundary value problem for the Helmholtz equation in cylindrical symmetry:

$$\nabla \cdot (r\nabla p) + k^2 r\, p = 0 \qquad \text{in } \Omega, \tag{1a}$$

$$\left(\mathrm{i}k + \frac{1}{R_\Omega}\right) p + \frac{\partial p}{\partial n} = 0 \qquad \text{on } \Gamma_{\text{out}}, \tag{1b}$$

$$\mathrm{i}kp + \frac{\partial p}{\partial n} = 2\mathrm{i}kA \qquad \text{on } \Gamma_{\text{in}}, \tag{1c}$$

$$\frac{\partial p}{\partial n} = 0 \qquad \text{on } \Gamma_n \cup \Gamma_{\text{sym}}, \tag{1d}$$

where p is the complex pressure amplitude field. (We assume an $\mathrm{e}^{\mathrm{i}\omega t}$ temporal behavior). Here n denotes the local normal at the boundary, r is the distance to symmetry axis, and ∇ and $\nabla\cdot$ are the two-dimensional gradient and divergence operators, respectively. Boundary condition (1c) specifies a right-going wave (towards the domain interior) of amplitude A at boundary Γ_{in} and absorbs all left-going waves (leaving the domain). Sound-hard and symmetry boundaries are described with boundary condition (1d), and Γ_{out} is an artificial boundary, where we apply the lowest order Engquist–Majda absorbing boundary conditions [3] to avoid reflections of out-going waves and thus to approximate the Sommerfelt radiation condition for the exterior wave propagation. Bängtsson et al. [1] discuss more about the boundary conditions.

The most notable idealization of the model is the omission of losses. In free air, losses are negligible for propagation over distances characteristic to e.g. a concert hall, but near boundaries viscous and thermal effects can be significant, especially for narrow waveguides. For the short and rather wide ducts at hand in the case of the loudspeaker horn, losses are of subordinate importance due to the relatively small area to volume ratio. This assumption has also been verified by calculating a rough check of the influence of losses using a one-dimensional transmission line model [6].

2.2 Optimization

Let η denote a set of *design variables* that specifies the actual shape of the horn flare. In this work we choose as design variables η the local *second derivative* of the horn flare function (*the horn flare function* is the distance from the horn boundary to a conical reference horn). This choice of design variables has the advantage of promoting smooth shapes without limiting the design flexibility and also makes it easy to impose convex shapes by constraining η to be of one sign [1].

The solution to Eq. (1) depends on the horn design through the shape of Ω, which in turn depends on the value of design variable η. To measure the transmission efficiency of a particular horn, we observe the *reflection coefficient* at boundary Γ_{in}. The reflection coefficient for a horn associated with design variable η and for a wave at frequency f can be defined as

$$R(f;\eta) = \frac{B}{A}, \tag{2}$$

where A and B are the complex amplitudes at Γ_{in} of the imposed (right-going) and reflected (left-going) waves, respectively. The horn design problem under consideration can then be formulated as the optimization problem

$$\begin{aligned} \min_{\eta} & \left[\sum_{f\in F} |R(f;\eta)|^2 + \frac{\epsilon}{2} \int_{\Gamma_d^{\text{ref}}} \eta^2 \, d\Gamma \right], \\ \text{s.t.} \quad & \eta \geq 0 \end{aligned} \tag{3}$$

where the second term is a (Tikhonov) *regularization term* and F is the set of frequencies for we minimize reflections. The inclusion of a regularization term makes it possible, if necessary, to balance the requirement of low reflections with the need for smooth shapes by adjustments of parameter $\epsilon \geq 0$. We use `lsqnonlin` in large-scale mode from Matlab's optimization tool box for optimization, where the gradient are supplied by the adjoint method. Udawalpola and Berggren [7] describe the optimization procedure in detail.

3 Experimental study

The purpose of the experimental study is to assess the validity of the design process, and to gain insight into its limitations in terms of modeling errors and the influence of the manufacturing tolerance.

3.1 The prototype

With the advent of different rapid manufacturing techniques, it has become possible to fabricate advanced shapes at low cost. For this project, an epoxy based stereo lithography technique (SLA) was used. Each layer in the printing process is 0.1 mm thick, effectively producing a staircase approximation of the intended shape. After sanding down the stairs, a final tolerance of around 0.2 mm is achieved.

The intention was to produce a prototype with roughly the same dimensions as existing 1.5" driver horns. However, in order to comply with the dimensions of available tubing used for the measurement system, the horn was scaled down by a factor of 0.93. The solution to the Helmholtz equation scales with the characteristic size (wave number to dimension) of the horn, but effects due to losses do not. As size decreases, the fraction of the acoustic field within the acoustic boundary layer becomes relatively larger. However, the scaling factor close to unit together with the already weak influence of damping, vouches for the validity of results also after the scaling.

It is usually desirable that the frequency band $[f_{\min}, f_{\max}]$ within which the horn is effective be as wide as possible. The choice of $f_{\min}$ and $f_{\max}$, is however to some extent subject to interactive adjustment. With the maximum dimensions of the horn given as a first design constraint, the limit for the functioning is quickly found from a set of initial design tests. As a rule of thumb, the horn is ineffective as an impedance matching for wavelengths above the length of the horn. By experimentation, it was found that $f_{\min} = 1.6$ kHz was a reasonable choice as a lower limit to obtain favorable transmission properties. Moreover, $f_{\max}$ was set at 9.05 kHz, which was mainly a limit imposed by numerical considerations. In purely acoustical terms, the value of $f_{\max}$ is usually not so critical, however, since the horn radiates efficiently quite regardless of its shape above the horn cutoff frequency. The frequency band 1.6–9.05 kHz over which the reflection is minimized is sampled at the 31 exponentially spaced frequencies $1600 \cdot 2^{m/12}$ Hz, where $m = 0, 1, \ldots, 30$[1]. Finite-element solutions of Eq. (1) were carried out using continuous, piecewise linear elements on a triangulation of domain Ω with a total of 49,701 degrees of freedom during the optimization step. For the post-optimization analysis, where the reflection spectrum associated with a computed design is evaluated more carefully, piecewise quadratic elements with 190,489 degrees of freedom are used. We use 231 design variables with a small amount of regularization, $\epsilon = 10^{-5}$, in the design study.

[1] The spacing corresponds to the notes of the equally-tempered scale.

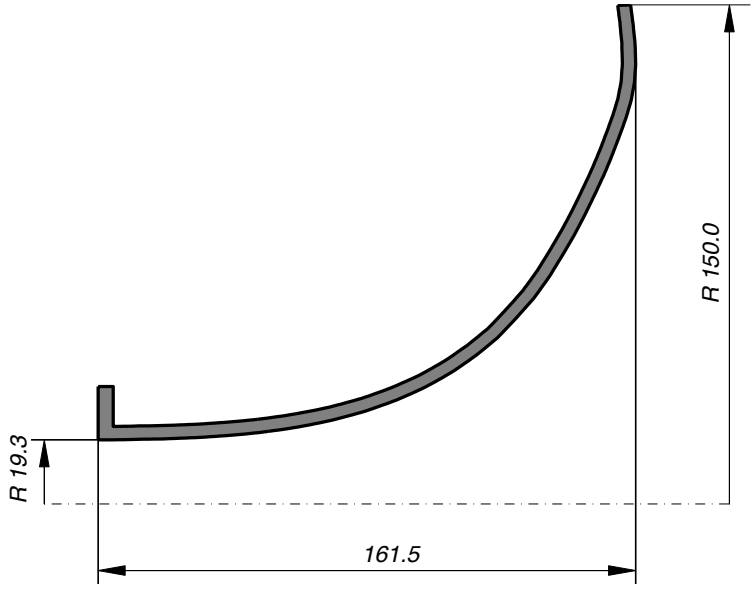

Figure 2: Drawing of the optimized horn.

A drawing of the computed optimal design can be seen in Fig. 2. The reflection spectrum, shown in Fig. 6, is flat over the design frequency range with a value that does not exceed 2%, except possibly at 1.6 kHz, where the curve slopes rapidly downwards. The finished horn prototype is shown in Fig. 3.

In a real horn, the driver is typically placed directly at the throat of the horn. The computations do, of course, consider higher modes, but the optimization is only made with regard to the planar mode. Inclusion of higher order mode information in the objective function is straightforward, if need be, but the low flare rate at the throat of the design found makes even the first radial mode of subordinate importance. For a driver–horn combination, it is likely that higher order modes near the driver are mainly a consequence of the membrane exhibiting a complex movement for high frequencies. This has been noted for real horns and has as a positive effect an increase in efficiency for high frequencies. In order to reduce the influence of higher modes excited by the flaring contour, the horn was attached to a 206.5 mm long cylindrical duct. In this way, evanescent modes generated by the horn are negligible at the measurement point. The cut-off frequency of the first radial mode is 11.7 kHz at room temperature. At 10 kHz, the same mode has decreased by a factor of $2.5 \cdot 10^{-10}$ over a distance of 200 mm, so it is safe to assume that influences of higher order modes stemming from the horn are of negligible importance. The length of the connecting duct was chosen in order to accommodate at least one wavelength at the design frequency low limit. This choice was made in order to prepare for an alternative measurement technique, whereby the standing wave ratio (SWR) is measured by moving a

probe microphone along the connecting duct.

The effect of geometrical deviations due to manufacturing deficiencies depends strongly on the position of the defect. If design constraints are not active, small deviations from the optimal profile can be expected to be of negligible effect, since perturbations of the objective function vanish to first order by definition of an unconstrained minimum. If constraints are active, the first order sensitivity to perturbations is in general not zero, though. Tests with different perturbation curves (constant positive or negative deviation of 0.2 mm, sinusoidal along the horn axis and with 0.2 mm amplitude) have shown that, at least for the tested perturbations, the effect on the impedance spectrum is less than 2 % for frequencies up to 6.5 kHz, but can be up to 8% near 8 kHz.

3.2 Measurement system

The reflection spectrum of an acoustic component can be measured in a variety of ways. In this project, the reflection spectrum was computed from the measured acoustic input impedance of the horn. The input impedance was measured using an impedance measuring head described by Dalmont et al. [2]. The system consists of a piezoelectric membrane with a cavity on one side, and an orifice on the other side. The membrane generates an acoustic signal, and by measuring the sound pressure via two microphones placed in the cavity and at the orifice, respectively, it is possible to calculate the input impedance of the object under investigation. The system has the advantage of ease of handling, and can be attached to objects with an entry diameter varying over a wide range of values. The system is also more easily characterized than systems based on an acoustic capillary. Once the input impedance $Z(f)$ of the horn is known, the complex reflection coefficient is given by the relation

$$R(f) = \frac{Z(f) - Z_0}{Z(f) + Z_0}.$$

In order to verify the performance of the measurement setup, an initial impedance measurement was performed on the cylindrical duct only. The duct is terminated by a small flange, and will show a large reflection for frequencies in the range of interest. Fig. 4 shows the results, where the measurements are compared with reflection coefficients computed using our finite-element method. Comparing the absolute value of the impedances, the curves agree on average within 1% in the band 1.0–6.0 kHz.

The measurements on the horn prototype were carried out in an anechoic chamber in order to minimize the influence of reflected waves and external noise. For systems with large reflections and correspondingly high internal sound levels such as in musical instruments, this is not such an important issue. A loudspeaker horn optimized for transmission has however the lowest possible internal sound pressure level for a given excitation, and is therefore potentially susceptible to disturbances.

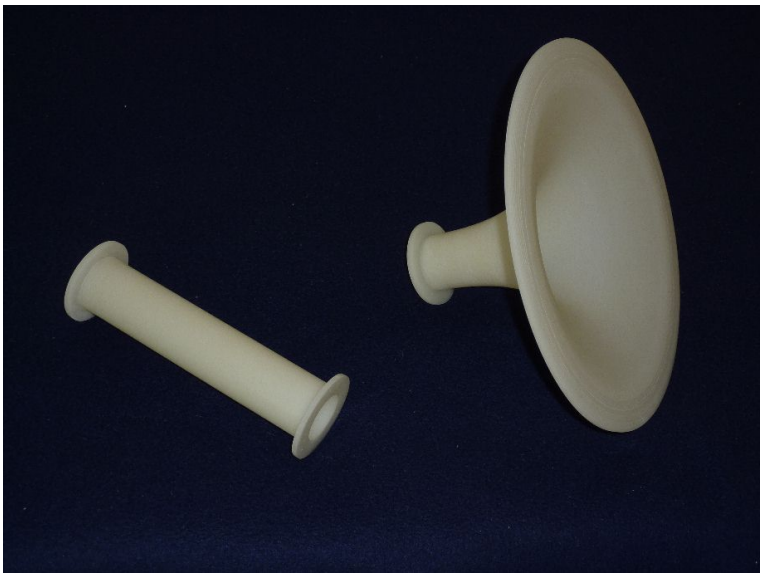

Figure 3: The horn prototype and the connecting duct.

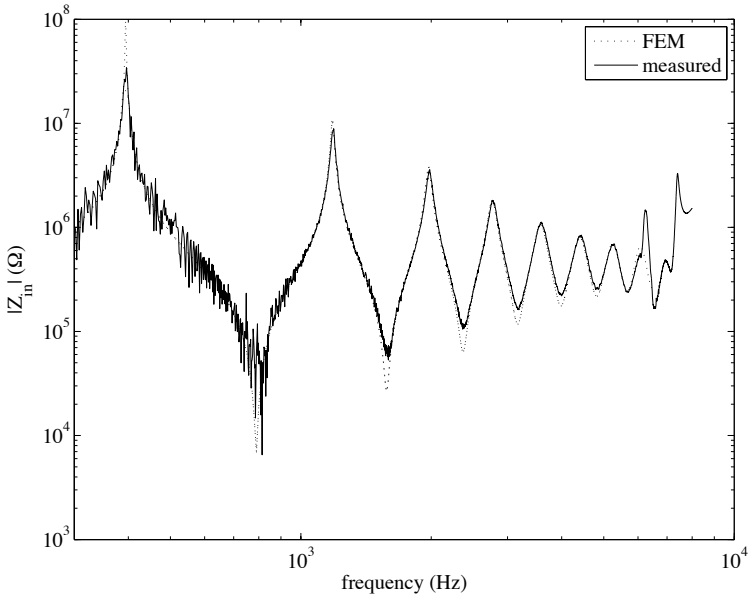

Figure 4: Input impedance for a cylindrical tube with a small flange.

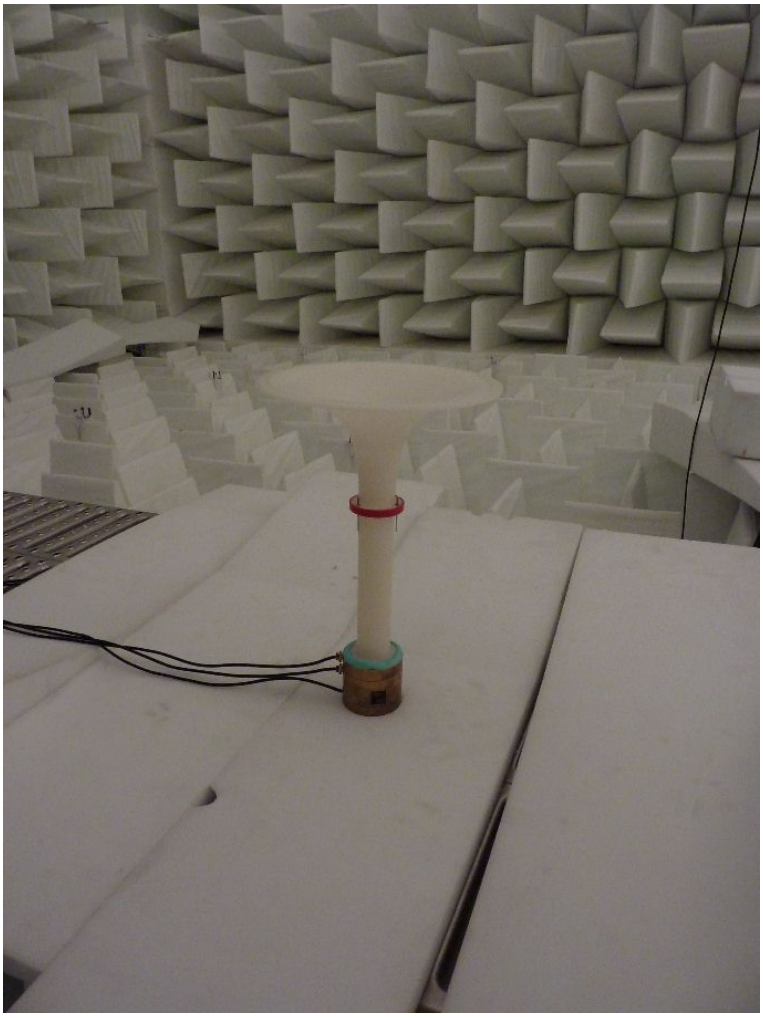

Figure 5: The horn prototype attached to the impedance head. Seen in the background are the foam wedges that cover the floor, walls, and the ceiling of the anechoic chamber.

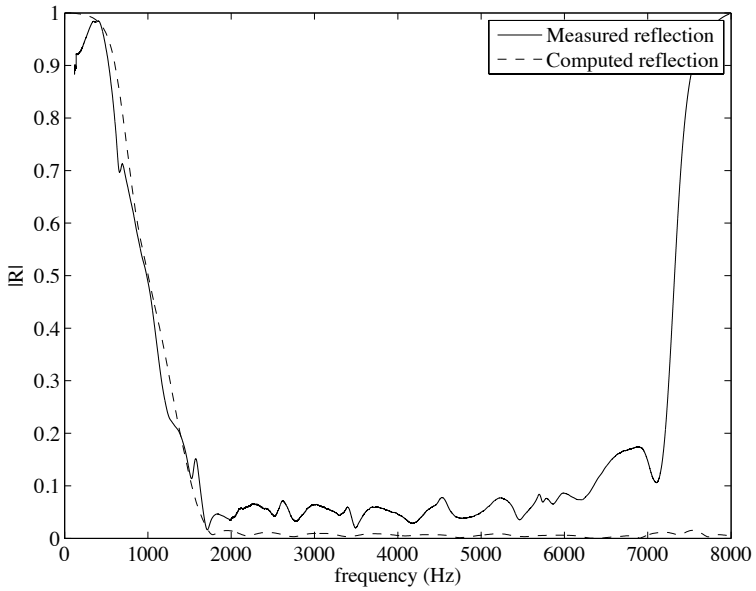

Figure 6: Measured and computed reflection spectra for the optimized horn.

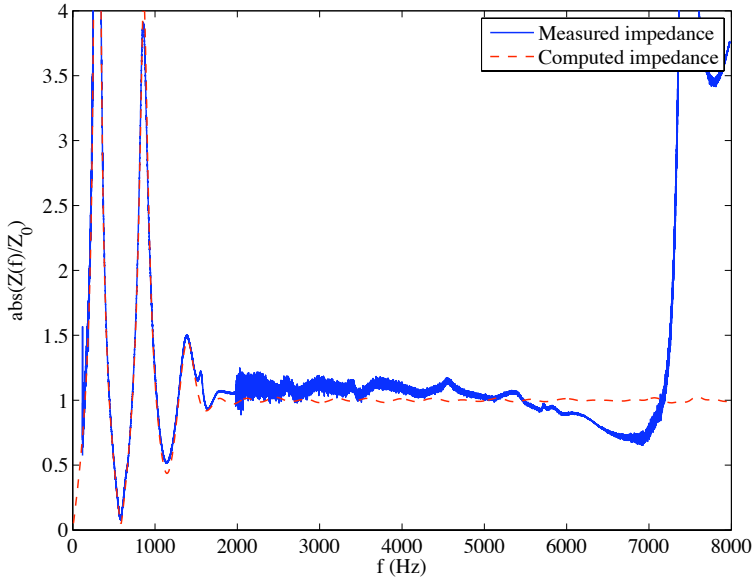

Figure 7: Computed and measured input impedance (normalized) of the optimized horn: modulus.

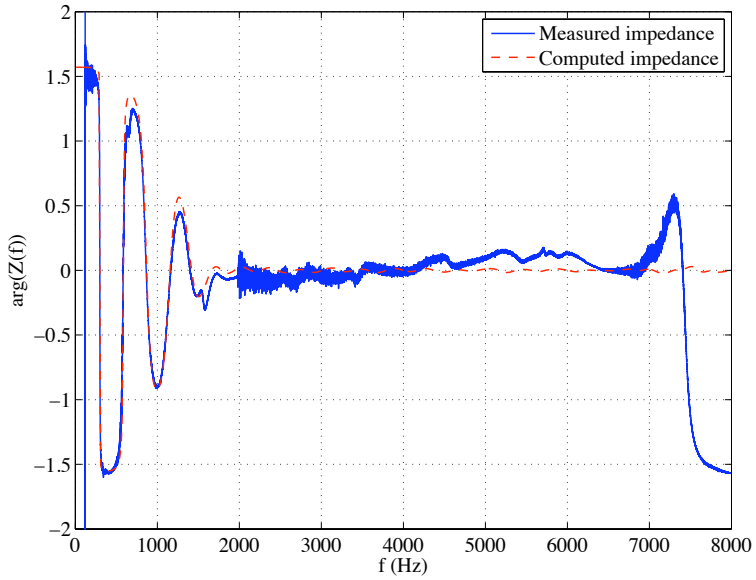

Figure 8: Computed and measured input impedance of optimized horn: argument.

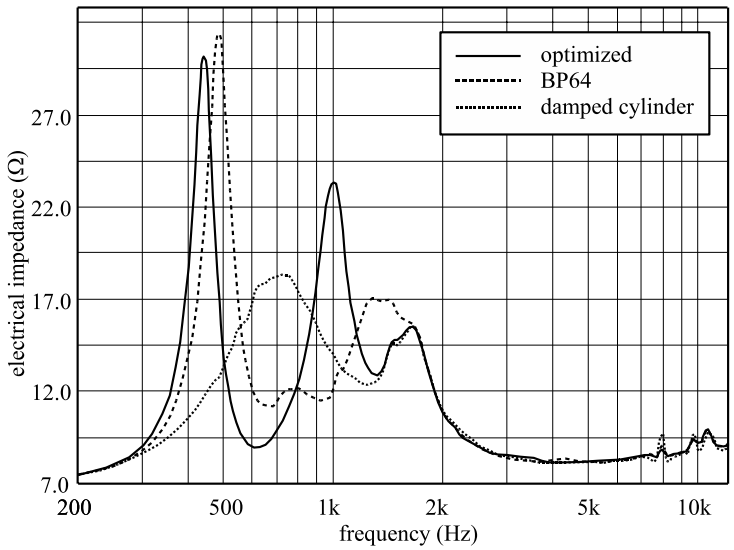

Figure 9: The electrical input impedance measured at the driver attached to the optimized horn (—), a horn in production (D.A.S. BP64)(- -), and to a damped cylindrical pipe (···).

3.3 Results

The measurement system parameters were selected as to yield maximum accuracy for frequencies above 1 kHz. The main compromise is the selection of signal strength, which varies with the frequency. Fig. 7–8 shows a comparison between the computed input impedance spectrum of the prototype and the measured one. The curves have been normalized by the characteristic impedance $\rho c/S$ of a waveguide of the same cross sectional area S as the horn throat. Here, ρ is the density of air and c the speed of sound. A perfect match is achieved when $Z_{\text{in}} = 1$. We see that the measured impedance is close to unity, although not perfectly so. According to the documentation of the instrument, around 2% can be attributed to uncertainties in the measurement system. We see that the measurements indicate a somewhat larger error than what might be expected considering the documented accuracy of the measurement system, and the errors due to the geometrical deviations mentioned in Sec. 3.1. The reason for this difference is note entirely clear, but a possible source of errors is the influence of higher modes around the orifice of the impedance measurement head. The diameter ratio between the horn throat and the orifice is rather large (3.6), and some localized radial motion is bound to take place. It is not clear to what extent this has been accounted for in the impedance measurement software. In terms of the reflection coefficient, the corresponding curves are shown in Fig. 6. The increasing deviation between measured and ideal data slightly above 6 kHz is in conformity with the observation that the system is locally more sensitive to manufacturing errors from 6.5 kHz. The trend is, however, masked just after 7 kHz where there is a resonance in the piezoelectric membrane of the impedance head.

In a loudspeaker configuration consisting of the horn and a driver, the acoustical input impedance of the horn influences the electrical impedance of the driver. Fig. 9 shows the input impedance of a D.A.S. M75-N driver attached to the transmission optimized horn and to the in-production horn D.A.S. BP64. It is seen that the impedance curves correspond over large parts of the design frequency band. In the lower part of the design frequency band, the electrical impedance is lower for the optimized horn, but this comes at the expense of the properties at frequencies just below f_{min}. The peak at 1 kHz corresponds with the second impedance peak of the optimized horn. The electrical impedance was also measured with the driver attached to a damped cylindrical pipe. Ideally, this pipe mimics the behavior of an infinite pipe with the constant impedance $\rho c/S$. We see that the impedance curve for the optimized horn is in close agreement with that of the damped pipe from around 1.25 kHz.

No data for the acoustic impedance of the BP64 horn were available, and the dependency of the electrical impedance on the acoustical loading of the driver is somewhat complicated, so we cannot presently make further quantitative statements.

4 Discussion and future outlooks

By automatic design tools, such as the one employed here, it is possible to find shapes that would otherwise be very difficult to find. Heuristic arguments are helpful in understanding acoustical phenomena in qualitative terms, but are of limited value for such highly sensitive problems as acoustical horn design. Although rapid manufacturing tools are becoming increasingly available, each produced unit is associated to a cost that gets considerable if multiple prototypes have to be made, not to mention the associated work. If a finely tuned horn is desired, automatic design is a prerequisite. The computational time for the presented design problem is in the order of a few hours on a personal computer, which makes the process tractable also for tailored design of specialized horns in limited series.

The main limitation of the presented tools is the restriction to two dimensions. Although not a source of errors under the chosen experimental conditions, the careful design of a practical loudspeaker whose shape or near surrounding deviates strongly from axisymmetry would probably need a three-dimensional model. The computational effort, which is completely manageable in two dimensions, quickly becomes prohibitively demanding in the three-dimensional case for a traditional finite element scheme. Current work employing different numerical schemes addresses this issue with the intention to develop design tools that useful for practical fully three-dimensional horn loudspeaker design.

Future work entails simultaneous optimization of the horn and the driver interior, notably the part commonly known as the phasing plug, which is in effect a part of the acoustical horn.

5 Acknowledgments

We are indebted to Eric Ogam and Fabrice Silva at Laboratoire de méchanique et d'acoustique, CNRS, for their kind assistance during the measurements.

References

[1] E. Bängtsson, D. Noreland, and M. Berggren. Shape optimization of an acoustic horn. *Comp. Meth. Appl. Mech. Eng.*, 192:1533–1571, 2003.

[2] J. P. Dalmont and J. C. Le Roux. A new impedance sensor for wind instruments. *J. Acoust. Soc. Am.*, 123(5):3014, 2008.

[3] B. Engquist and A. Majda. Absorbing Boundary Conditions for the Numerical Simulation of Waves. *Math. Comp.*, 31:629–651, 1977.

[4] M. B. Giles and N. A. Pierce. An introduction to the adjoint approach to design. *Flow Turbul. Combust.*, 65:393–415, 2000.

[5] J. Kemp, J. Chick, M. Campbell, and D. Hendrie. Acoustic pulse reflectometry for the measurement of horn crooks. In *Acoustics'08*, pages 519–524, Paris, June–July 2008.

[6] D. Mapes-Riordan. Horn Modeling with Conical and Cylindrical Transmission-Line Elements. *J. Audio Eng. Soc.*, 41:471–483, 1993.

[7] R. Udawalpola and M. Berggren. Optimization of an acoustic horn with respect to efficiency and directivity. *Int. J. Num. Meth. Eng.*, 73(11):1571–1606, 2008.

[8] E. Wadbro, R. Udawalpola, and M. Berggren. Shape and topology optimization of an acoustic horn–lens combination. *J. Comput. Appl. Math.*, 2009. In press, corrected proof available online.